Ethanolysis of Glucose into Biofuel 5-Ethoxymethyl-Furfural Catalyzed by $NH_4H_2PO_4$ Modified USY Zeolite

Yihang Chen,[a] Xuanyu Liang,[a] Kutumova Aliya,[a] Zhangbin Zheng,[a] Chao He,[a] Youzhou Jiao,[a] Hongge Tao,[a] Chun Chang,[b] and Guizhuan Xu [a,c,*]

5-Ethoxymethylfurfural (EMF) can be considered as a potential biofuel because of its excellent combustion properties, such as high energy density and low carbon smoke emissions. In this study, Ultra-stable Y (USY) zeolite was modified with $NH_4H_2PO_4$ and then used as an efficient solid catalyst for the catalytic synthesis of EMF *via* ethanolysis of glucose First, the $NH_4H_2PO_4$-modified USY was characterized by FT-IR, XRD, BET, and NH_3-TPD. The effect of reaction temperature, reaction time, substrate concentration, and catalyst loading on the yield of EMF was investigated. The P0.2-USY optimal EMF yield was 39.6 mol%, which increased by 20.7% compared to USY, and still had better activity after being reused for 5 cycles. Moreover, the pseudo-homogeneous first-order kinetics model was developed to elucidate the kinetics of EMF formation from glucose, and the kinetics results showed that the activation energy of EMF formation (64.2 $kJ \cdot mol^{-1}$) was lower than that of humins formation (73.2 $kJ \cdot mol^{-1}$). Finally, the ethanolysis pathway was proposed based on the product distribution.

DOI: 10.15376/biores.18.2.2707-2725

Keywords: 5-Ethoxymethylfurfural; Ethanolysis; Kinetics; Pathway

*Contact information: a: College of Mechanical and Electrical Engineering, Henan Agricultural University, Zhengzhou 450002, China; b: School of Chemical Engineering, Zhengzhou University, Zhengzhou 450001, China; c: Henan Key Laboratory of Green Manufacturing of Biobased Chemicals, Puyang 457000, China; * Corresponding author: xuguizhuan@henau.edu.cn*

INTRODUCTION

Fuels and chemicals are indispensable products for modern society, and they are mainly produced from non-renewable fossil resources (Gómez Millán *et al*. 2019a). With the decline of fossil resources and growing environmental problems, the development of renewable energy sources is imperative (Gómez Millán *et al*. 2019b; Wu *et al*. 2020). Lignocellulose, as an abundant and inexpensive neutral carbon source, can be converted into high-value platform chemicals and biofuels, such as xylitol, furfural, glucaric acid, 5-hydroxymethylfurfural (5-HMF), ethyl levulinate(EL), 2,5-furandicarboxylic acid (FDCA), *etc.* (Chen *et al*. 2020a; Liu and Abu-Omar 2021; Liu *et al*. 2021; Peixoto *et al*. 2021). As a new chemical and biofuel, 5-ethoxymethylfurfural (EMF) has attracted much attention. EMF has an energy density of 30.3 $MJ \cdot L^{-1}$, which is similar to that of gasoline (31.9 $MJ \cdot L^{-1}$). It has excellent combustion properties, such as high oxidative stability and low toxicity, which could reduce exhaust gases, smoke emissions, and particulate pollution (Li *et al*. 2016a,b; Xu *et al*. 2017; Liu and Wang 2019). Additionally, EMF can be used as a flavor and aroma additive in food and beverage (Liu and Wang 2019).

As an abundant and inexpensive monosaccharide, glucose is an ideal raw material for EMF production *via* one-pot ethanolysis. During ethanolysis, the catalyst is essential

for the cascade reactions of glucose isomerization to fructose, fructose dehydration to HMF, and HMF etherification to EMF (Zheng *et al*. 2021; Wang *et al*. 2021; Wang *et al*. 2022a). Liquid or solid acid catalysts can be used. Although liquid acids are widely available and inexpensive, they can cause equipment corrosion and environmental pollution, and they are difficult to recover and reuse (Balakrishnan *et al*. 2012). Solid acid catalysts have the advantages of being separated easily from the reaction, not corroding equipment, superior recyclability, and excellent thermal stability. Thus, the application of solid acid catalysts in EMF production is a research hotspot (Zhang and Huber 2018).

Solid acid catalysts used in EMF production mainly include zeolites, heteropolyacid-based hybrid catalysts, and sulfonate functionalized catalysts, as well as some others (Wang *et al*. 2017; Nie *et al*. 2022). Zeolites are molecular sieve catalysts, which are natural or synthetic chemicals with a network structure consisting of highly dispersed microporous channels (Chen *et al*. 2019). However, the unique micropore structure of molecular sieves restricts the diffusion of reactants and affects the catalytic performance (Liu and Wang 2018). The modification of zeolite to change the pore size and acid sites is important for biomass conversion reactions. Bai *et al.* (2018) reported the application of hierarchical meso-/microporous lamellar MFI-Sn/Al zeolites in EMF production. The MFI-Sn/Al zeolites contained both Lewis acidic Sn and Al sites and Brønsted acidic Al-O(H)-Si, which catalyzes the conversion of glucose to EMF with a yield of 44%. Rao *et al.* (2020) produced sufficient Brønsted and Lewis acidic sites in SBA-15 by loading tin-modified heteropoly silicate (SnSTA), resulting in 41% EMF yield from glucose and 72% EMF yield from fructose. Morales *et al.* (2017) modified SBA-15 with aromatic sulfonic acid to catalyze the glucose conversion in a dimethyl sulfoxide (DMSO)/ethanol medium at 116 °C for 4 h, with an EMF yield of 63.4%. Although some progress has been made in the preparation of EMF from glucose using modified catalysts, the concentration of substrate is usually low (≤50 g/L), and the reaction time is long (≥ 1 h) (Morales *et al*. 2017). Therefore, it is important to develop efficient solid acid catalysts suitable for high substrate concentration.

The ratio of Lewis acid to Brønsted acid is an important factor in EMF selectivity (Yu *et al*. 2021). It might be an effective strategy to promote EMF production by regulating the ratio of Lewis / Brønsted acid of solid acid catalysts. Ultra-stable Y (USY) zeolite is an efficient solid acid catalyst for EMF synthesis (Zheng *et al*. 2021; Wang *et al*. 2022a). Modification of USY is expected to improve the EMF production from biomass. Sulfuric acid, nitric acid, phosphoric acid, and citric acid have been used to modify USY. Phosphoric acid and nitric acid adjust the micropore and mesopore distribution of USY, and citric acid increases the L acid content of USY (Heda *et al*. 2020; Pande *et al*. 2018).

Preliminary experiments showed that USY modified by ammonium dihydrogen phosphate ($NH_4H_2PO_4$) has a positive effect on the ethanolysis of fructose. EMF yield was 82.3%, which was increased by 11.6% Inspired by this result, the $NH_4H_2PO_4$-modified USY was generated to promote the ethanolysis of glucose for EMF production (Scheme 1). In this work, the characteristics of modified USY and its catalytic performance on the EMF formation from glucose were investigated. A pseudo-homogeneous first-order kinetics model was developed to elucidate the kinetics of EMF formation. Possible reaction pathways were proposed based on the product distribution. This study inspires EMF production by ethanolysis of lignocellulosic biomass.

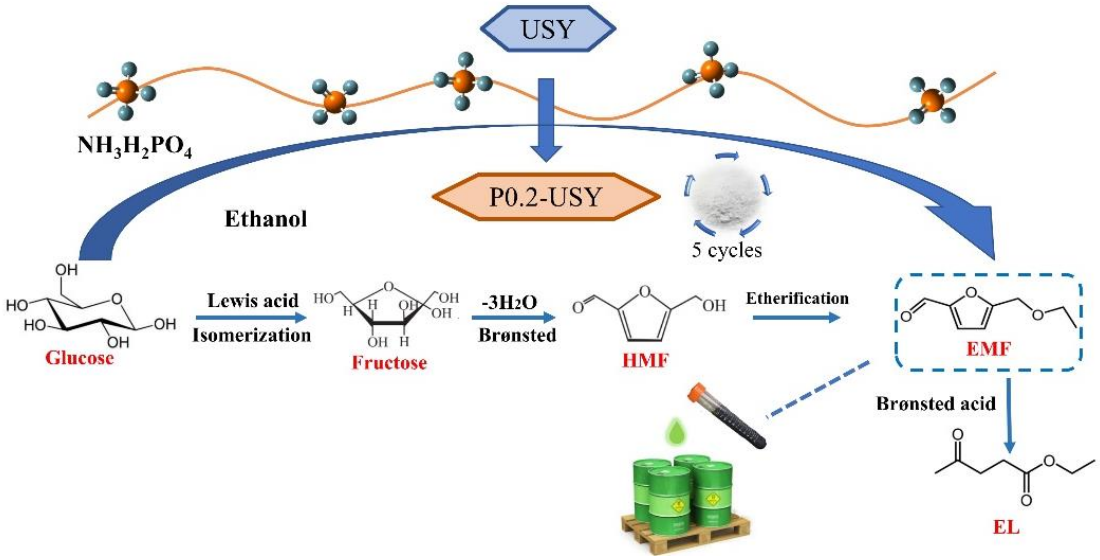

Scheme 1. P0.2-USY-catalyzed glucose alcoholysis

EXPERIMENTAL

Materials

Glucose (>99%), fructose (>99%), cellulose (>99%), EL (>99%), and HMF (>98%) were purchased from Aladdin Reagent (Shanghai, China). Corn stover was provided by a local farm (Zhengzhou, China). EMF (>97%) was obtained from Sigma-Aldrich (Shanghai, China). USY (NKF-7II) was purchased from Nankai University Catalyst Co., Ltd (Tianjin, China); the surface area, Si/Al ratio, and Na_2O content of USY were 600 $m^2 \cdot g^{-1}$, 5.3, and 1.8 wt%, respectively. $NH_4H_2PO_4$ (>99%) and ethanol with chemical purity were bought from Sinopharm Chemical Reagent Co., Ltd. (Shanghai, China).

Preparation of Modified USY

The modified substances were loaded on USY by the impregnation method. First, 1.0 g of USY was added to 20 mL of $NH_4H_2PO_4$ aqueous solution with different concentrations. It was macerated at 25 °C for 2 h, filtered, and washed three times with deionized water. The catalyst was dried at 105 °C for 4 h. The dried catalyst was calcined at 550 °C for 4 h, cooled, and collected.

Characterization of Catalyst

A Bruker D8 Advance XRD diffractometer (Karlsruhe, Germany) was used to characterize the crystal structure of the USY solid molecular sieve. The samples were tested under Cu Kα radiation source with the following conditions: tube current of 35 mA, tube voltage of 40 kV, diffraction angle 2θ ranging from 4 to 60°, and scanning speed of 3°/min. The changes in functional groups before and after the catalyst modification were analyzed using a Fourier-transform infrared (FTIR) (iS10 Nicolet-IR 200, Madison, WI, USA) spectrometer with 4 cm^{-1} resolution, and the scanning range was from 400 to 4000 cm^{-1}. The pore volume, pore size, and specific surface area of the catalysts were analyzed using a fully automated BELSORP mini II specific surface area and porosity analyzer

(Osakan Kaupunki, Japan). The catalyst was characterized using a micropolitics Auto Chem II 2920 fully automated programmed temperature rise chemisorption instrument (Norcross, GA, USA). A tensor 27 Fourier infrared spectrometer (Bruker) was used to characterize the B/L acid amounts of the USY samples.

Ethanolysis of Glucose

A certain amount of glucose and catalyst were mixed with 40 mL (40% of the maximum capacity of the reactor) of anhydrous ethanol and placed in an autoclave with a magnetic stirring device, sealed, and heated. The stirring speed was kept at 250 rpm during the heating phase to mix the substrate with the solvent and catalyst. When the temperature reached the set temperature, the time was set to zero and the stirring speed was adjusted to 500 rpm. At the end of the ethanolysis reaction, the reactor was placed in a cold water bath to terminate the ethanolysis reaction. The solid and liquid phases of the reaction products were separated by vacuum filtration and the liquid phase was filtered using a 0.45 μm filter for further analysis.

Products Analysis

EMF, fructose, and glucose were quantified by high-phase liquid chromatography (HPLC) equipped with a refractive index detector (RID), HPX-87H (300 mm × 7.8 mm) with a mobile phase of 0.005 mol·L^{-1} sulfuric acid solution, a column temperature of 65 °C, and a flow rate of 0.6 mL/min. GC equipped with a flame ionization detector and a TG-5MS capillary column was used to test EL, and the temperature program was, the initial temperature 60 ℃, holding for 3 min, ramping up to 240 ℃ with a rate of 10 ℃/min, and then holding 8 min, and then ramping up to 280 ℃, holding for 2 min with a rate of 10 ℃/min. The inlet temperature and detector temperature were both 250 ℃, and the carrier gas was nitrogen with a rate of 1.0 mL/min. The EL was determined by the internal standard method, and 200 mg/L of n-octanol was selected as the internal standard compound to prepare EL standard solutions of different concentrations. The EL standard solutions were determined according to the above chromatographic conditions as well as the method, respectively. Under the above gas chromatographic conditions, the retention time of EL was about 8.9 min, and that of the internal standard compound n-octanol was 8.1 min. The linear regression equation was derived from the concentration ratio and peak area ratio of EL and n-octanol at different concentrations, and according to the regression equation, the EL concentration was obtained. The liquid products distribution was performed on GC-MS, with an HP-5MS capillary column (30 m × 0.32 mm × 0.50 μm), and a flame ionization detector (Agilent Technologies 7890B, USA). The temperature program was, initial temperature 40 °C for 2 min, ramping up to 220 °C at a rate of 10 °C/min for 8 min, and helium was used as carrier gas.

The conversion of glucose, the yield of EMF, and the yield of EL were calculated by Eqs. 1, 2, and 3, respectively.

$$Conversion\ of\ glucose\ (mol\%) = \frac{Moles\ of\ initial\ glucose - Moles\ of\ residual\ glucose}{Moles\ of\ initial\ glucose} \times 100 \quad (1)$$

$$Yield\ of\ EMF\ (mol\%) = \frac{Moles\ of\ EMF\ detected}{Moles\ of\ initial\ glucose} \times 100 \quad (2)$$

$$Yield\ of\ EL\ (mol\%) = \frac{Moles\ of\ EL\ detected}{Moles\ of\ initial\ glucose} \times 100 \quad (3)$$

RESULTS AND DISCUSSION

Screen and Characterization of Catalyst

USY zeolite was modified by different $NH_4H_2PO_4$ loadings in the experiments, and the catalytic performance of USY and modified USY on the EMF yield was first investigated. Figure 1 shows that EMF yield increased with the increase of the $NH_4H_2PO_4$ concentration. The USY modified by 0.2 wt.% concentration of $NH_4H_2PO_4$ showed a good catalytic performance. When the $NH_4H_2PO_4$ concentration was more than 0.2 wt.%, the higher concentration resulted in a lower EMF yield. Therefore, 0.2 wt.% can be used as a suitable $NH_4H_2PO_4$ concentration, and the modified USY named P0.2-USY was screened as the optimal modified catalyst for further investigation.

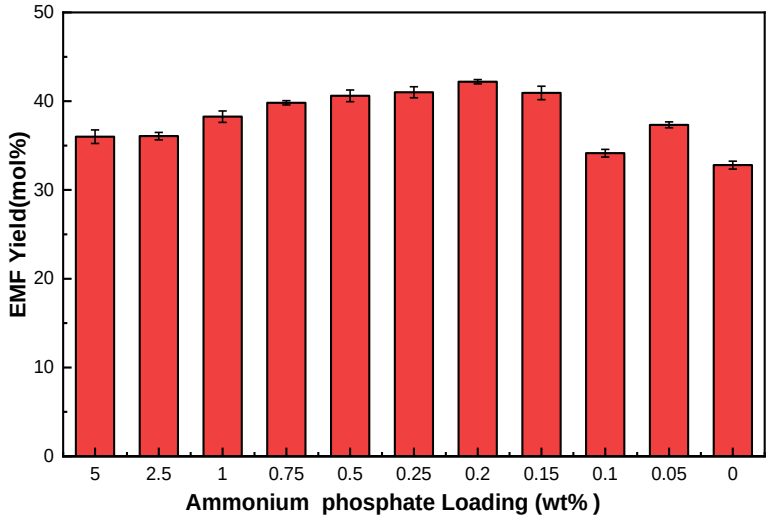

Fig. 1. Effect of modified USY with different $NH_4H_2PO_4$ on EMF yield. Reaction conditions: 60 mL ethanol, 100 g·L^{-1}, 200 °C, 10 min, 1.8 wt.%

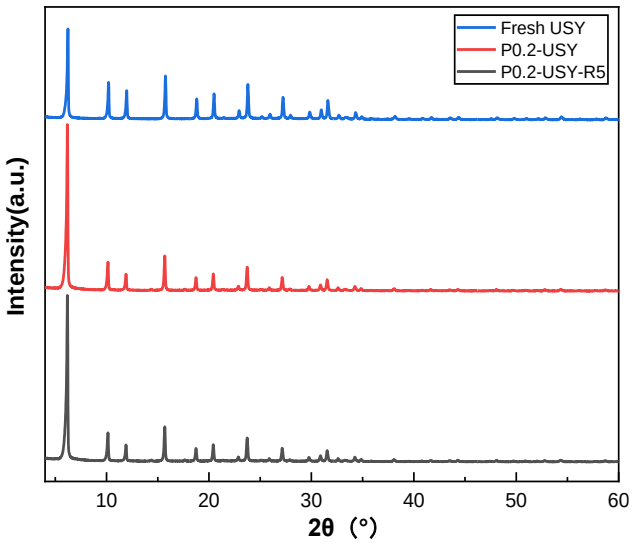

Fig. 2. X-ray diffraction of catalyst

USY and the modified P0.2-USY were analyzed by XRD. As shown in Fig. 2, characteristic peaks at 10.16°, 11.92°, 15.68°, 18.74°, 20.46°, 23.74°, and 27.16° were

observed (Li *et al*. 2014). These identical peaks suggested that the structure of the catalysts did not change. There was a slight decrease in the peak height of modified P0.2-USY, which was likely due to reduced crystallinity and a partial collapse of the USY framework structure caused by calcination (Pande *et al*. 2018; García *et al*. 2016).

The physical parameters of the catalysts were analyzed by the BET method, and the results of pore volume, pore size, and specific surface area are shown in Table 1. The pore size of the USY was changed from 0.6 nm to 0.7 nm after modification. The pore volume slightly increased (1.9%), while the specific surface area was reduced by approximately 2%.

Table 1. BET Analysis Results of Catalyst

Catalyst	Pore volume ($cm^3 \cdot g^{-1}$)	Pore radius (nm)	Surface area ($m^2 \cdot g^{-1}$)
USY	0.3836	0.6	841
P0.2-USY	0.3907	0.7	827.54

The FTIR spectra of P0.2-USY and USY are shown in Fig. 3. The catalyst showed a characteristic peak of the surface hydroxyl group between 3400 and 3450 cm^{-1}. The peaks observed at 1045, 790, and 450 cm^{-1} are Si-O bonds in zeolites (Buttersack and Laketic 1994), where the peak at 1045 cm^{-1} is an O-Si-O asymmetric stretching vibration peak (Kim *et al*. 2011; Verboekend *et al*. 2012). There was no obvious change in the position of the characteristic peaks, indicating that the silica-alumina ratio of the molecular sieve was unchanged with the modification.

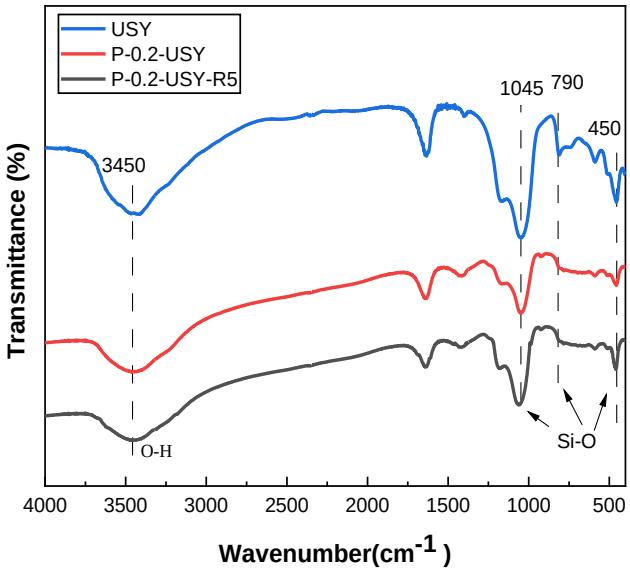

Fig. 3. FT-IR spectra of catalyst

The NH_3-TPD spectra of USY and P 0.2-USY are shown in Fig. 4. The desorption peaks between 150 and 250 °C characterize the weak acid center, and the desorption peaks between 350 and 450 °C characterize the medium to strong acid center. The central temperature of the weak acid center changed from 183.2 to 197 °C after modification, and that of the strong acid center changed from 398.6 °C to 405.7 °C after the modification. The shift of temperatures indicated that P0.2-USY adsorbed ammonia more strongly after

modification compared to USY, reflecting that the modified substance enhanced the acidity of USY. The peak of P0.2-USY was much higher than that of USY also confirmed the result.

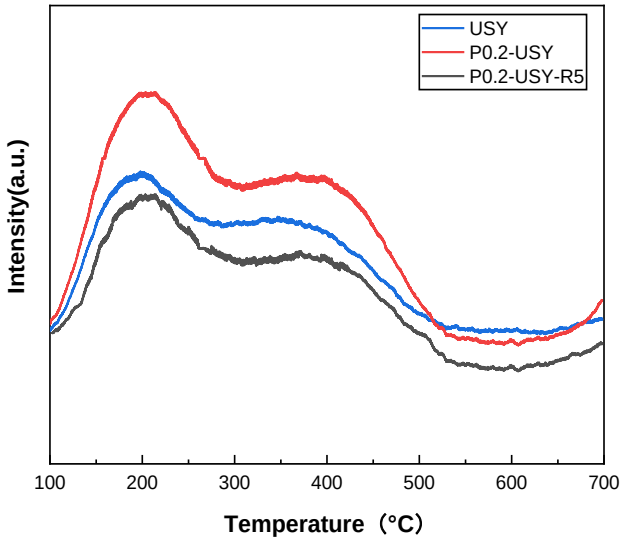

Fig. 4. NH_3-TPD spectra of catalyst

Py-IR results of USY and P0.2-USY are shown in Fig. 5. The absorbance peak located at 1540 cm^{-1} was the typical Brønsted acid peak (Fals *et al*. 2020), and the absorbance peak at 1450 cm^{-1} corresponded to Lewis acid (Oruji *et al*. 2018). The peak around 1490 cm^{-1} was formed by pyridine adsorption in Brønsted acid and Lewis acid (García *et al*. 2016; He *et al*. 2022). The ratio of Lewis/Brønsted acid increased from 0.51 to 0.82 for weak acids (200 °C), and 0.19 to 0.36 for medium strong acids (350 °C) (Table 2).

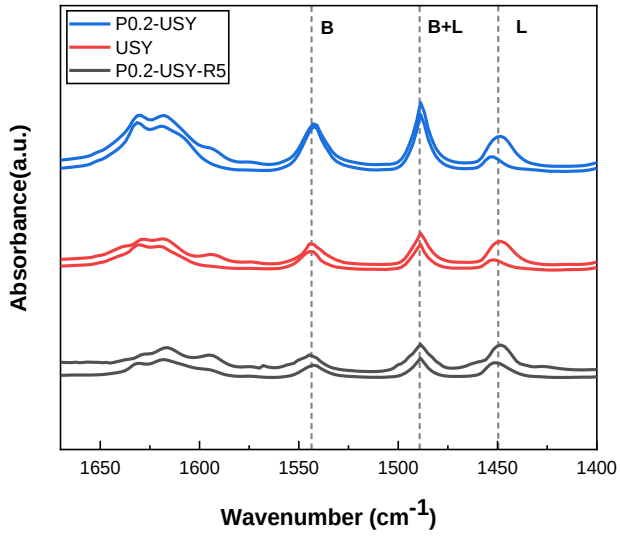

Fig. 5. Py-IR spectra of catalyst

Table 2. Py-IR Analysis Results of Catalyst

Catalyst	The ratio of Lewis acid to Bronsted acid	
	200 °C	350 °C
USY	0.51	0.19
P0.2-USY	0.82	0.36
P0.2-USY-R5	1.03	0.45

Effects of Reaction Conditions on Glucose Ethanolysis

The effects of reaction conditions on glucose ethanolysis, including EMF, fructose, EL yield, and glucose conversion, are shown in Fig 6. The effect of catalyst dosage was investigated first, and the result was shown in Fig. 6a. Within the range of catalyst dosage of 1.65% to 2.25%, glucose conversion was nearly 100%, indicating that glucose reacted thoroughly at the catalyst dosages. However, the yield of EMF and EL increased with the increase of catalyst dosage from 1.65% to 1.95% and decreased with the increase of catalyst dosage from 1.95% to 2.25%.

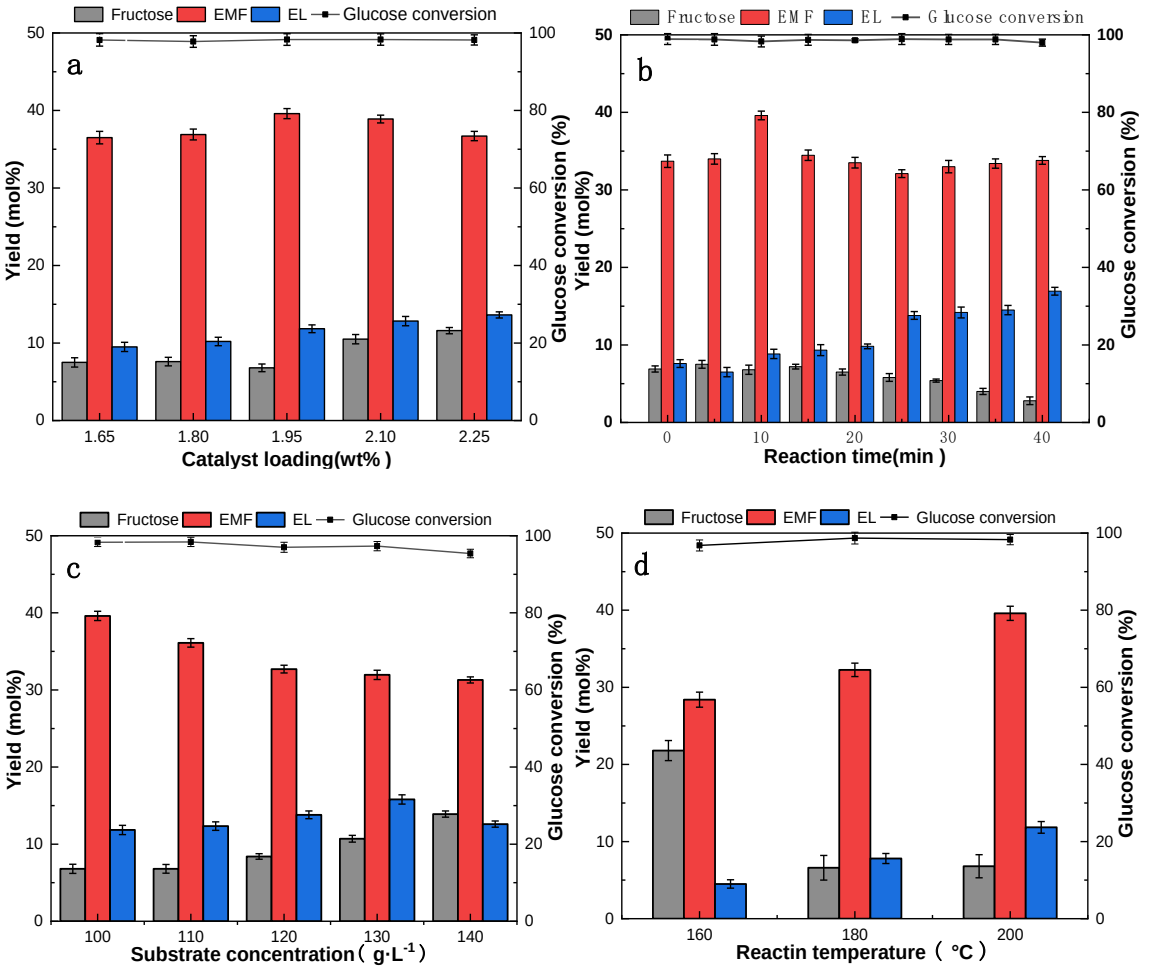

Fig. 6. Effect of reaction conditions on the conversion of glucose to EMF catalyzed by P0.2-USY. Reaction conditions: 60 mL ethanol. (a) Substrate concentration 100 g·L^{-1},200 °C, 10 min, (b) substrate concentration 100 g·L^{-1}, 200 °C, P0.2-USY 1.95 wt%, (c) 200 °C, 10 min, P0.2-USY 1.95 wt%, (d) 10 min, substrate concentration 100 g·L^{-1}, P0.2-USY 1.95 wt%

When 1.95% of the catalyst was used, the EMF yield increased to a maximum value of 39.6 mol% and the yield of EL increased to 12.5 mol%. Similarly, fructose content increased with the catalyst dosage increasing from 1.95% to 2.25%. The presence of fructose indicated that there was still fructose isomerized from glucose unreacted under the reaction conditions.

The effect of reaction time on glucose alcoholysis to EMF is shown in Fig. 6b. The EMF yield was approximately 32 mol% at zero time. The glucose conversion was 100% and constant with the further passage of reaction time. After a short reaction time of 10 min, the highest EMF yield of 39.6 mol% was achieved. After that, the yield of EMF decreased sharply at 15 min and maintained nearly the same value from 15 to 40 min, indicating that a short reaction time of 10 min was sufficient for EMF synthesis from glucose catalyzed by the modified USY. Furthermore, the fructose yield increased when the reaction time increased from zero to 25 min, suggesting that the isomerization of glucose to fructose was likely to have occurred within 25 min. However, the yield of EL grandly increased as the reaction time increased, indicating that the extension of reaction time was favorable for EL accumulation (Wang *et al*. 2022b).

The effect of substrate concentration on the reaction is shown in Fig. 6c. To realize the ethanolysis of glucose with high substrate concentration to prepare EMF, a high substrate concentration range from 100 to 140 $g \cdot L^{-1}$ was chosen for the ethanolysis experiments. As shown in Fig. 6c, both the EMF yield and glucose conversion gradually decreased with the increase of the substrate concentration, and the maximum yield of EMF and glucose conversion can be achieved at a substrate concentration of 100 $g \cdot L^{-1}$. Contrarily, the fructose content increased with the increase in substrate concentration, indicating that more fructose was produced. EL yield increased as the substrate concentration increased from 100 to 130 $g \cdot L^{-1}$. However, when the substrate concentration was 140 $g \cdot L^{-1}$, the EL yield decreased significantly, which might be caused by insufficient acid sites in the reaction system.

The effect of reaction temperature on glucose alcoholysis is illustrated in Fig. 6d. The EMF yield increased when the temperature was increased from 160 to 200 °C, and the maximum EMF yield was obtained at 200 °C. The glucose conversion was nearly constant from 160 to 200 °C. Similarly, the EL yield increased with the increase in temperature, indicating that high temperature can promote the synthesis of EL. However, the content of fructose decreased sharply as the temperature increased. Based on the above results, the optimal reaction conditions for glucose ethanolysis into EMF catalyzed by P0.2-USY were 1.95 wt.% of catalyst dosage, 100 $g \cdot L^{-1}$ of substrate concentration, reaction temperature 200 °C, and reaction time 10 min. Under the optimal reaction conditions, the maximum EMF yield was 39.6 mol%, which increased by 20.7% compared with the result catalyzed by USY (32.8 mol%).

The catalytic performance of modified Y-type zeolite (P0.2-USY) was tested using other biomass derivatives as substrates (Table 3). The EMF yield of fructose (82.3%) was significantly higher than that of glucose (39.6%). The fructose conversion to EMF is formed by Brønsted acid-driven dehydration, while the isomerization of glucose to fructose is a Lewis-catalyzed reaction and is the rate-limiting step (Wang *et al*. 2022a). Due to the van der Waals forces, and intermolecular hydrogen bonding that cellulose has, chemical bond breaking is more difficult (Peixoto *et al*. 2021). The main components of corn stover are holy carbohydrates and lignin, and the structure is difficult to destroy. P0.2-USY catalyzed corn stover can still obtain 10.8% EMF.

Table 3. Product Distribution From the Conversion of Different Substrates Over the P0.2-USY

Substrate	Conversion (%)	Yield (mol%)	
		EMF	EL
Fructose[1]	100	82.3	7.3
Glucose	97.2	39.6	11.8
Cellulose[2]	61.2	16.3	4.7
Corn straw[3]	34.6	10.8	2.4

[1]Reaction conditions: 120 °C, 30 min, 40 g/L, 1.5 wt%.
[2]Reaction conditions: 200 °C, 120 min, 20 g/L, 1.9 wt%.
[3]Reaction conditions: 180 °C, 150 min, 15 g/L, 2 wt%.

Reusability and Characterization of P0.2-USY

The reusability of the P0.2-USY zeolite catalyst was tested by cyclic tests. After the reaction, the catalyst was filtered and recovered, dried overnight at 105 °C, and roasted at 500 °C for 4 h in a muffle furnace. As shown in Figure 7, the EMF yield was 28.6% after 5 repetitions, showing the good catalytic activity of P0.2-USY. The decrease in EMF yield may be due to the reduced P0.2-USY pore space and the loss of acid sites. The characterization of catalyst P0.2-USY-R5 was performed, and no significant changes in grain size and morphology were observed after 5 cycles (Figures 2 and 3). As shown in Fig. 4, the change in the acidity of P0.2-USY after recycling was characterized by NH_3-TPD. Both the weak and strong acid peaks decreased after reused for 5 cycles of P0.2-USY, indicating the loss of acid sites. The result was also verified by Py-IR, as shown in Fig. 5. Both Lewis acid and Brønsted acid sites were reduced, which is one of the reasons for the decrease in catalytic activity. The Lewis/Brønsted ratio increased (Table 2), which is due to the loss of more Brønsted acid.

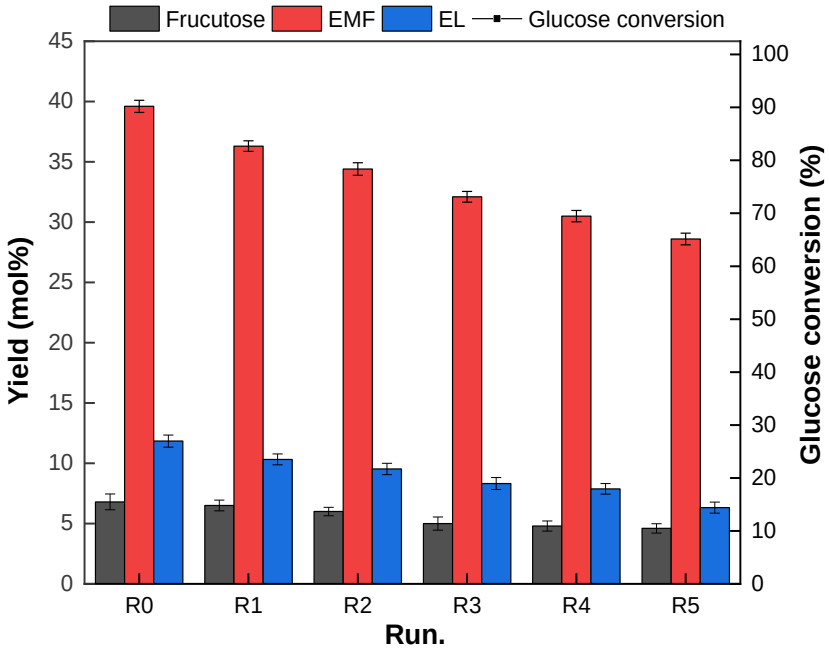

Fig. 7. Reusability of catalyst; reaction conditions: 200 °C, 100 g/, 10 min, catalyst dosage 1.95 wt%

Catalytic Pathway

To elucidate the reaction pathway of the glucose methanolysis into EMF catalyzed by P0.2-USY, GC-MS was used to identify the products, and the results are shown in Fig. 8. The identified components are shown in Table 4.

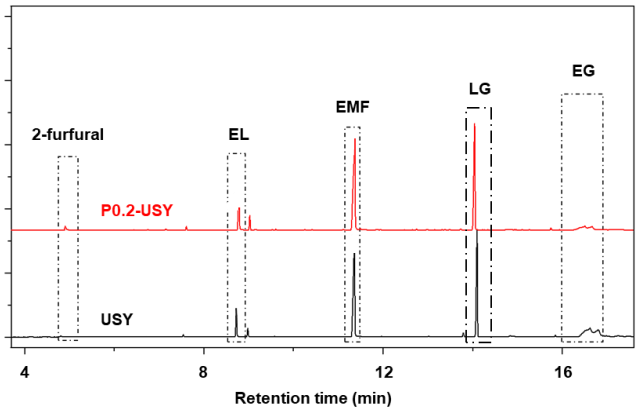

Fig. 8. GC-MS atlas of glucose products

The liquid phase products catalyzed by USY and P0.2-USY were mainly EMF, EL, 1,6-anhydro-β-D-glucose (LG), and ethyl-D-glucopyranoside (EDGP). Based on the previous reports, three reaction routes for the ethanolization of glucose to EMF were summarized, as shown in Fig. 9. In path I, glucose was isomerized to fructose by Lewis acid, and fructose was dehydrated and converted to HMF, and then etherified to EMF, which was also the main reaction route in the process of glucose ethanolysis (Tao *et al.* 2021). According to path II, glucose was firstly converted to EDGP, and then it was isomerized to ethyl-D-fructofuranoside (EDFF), which will then be etherified into EMF (Liu and Wang 2018). Besides, one can consider path III, in which glucose isomerization to fructose is reacted with ethanol in an acidic solution to generate EDFF, then dehydration to produce EMF (Zhang *et al*. 2018). Based on GC-MS results (Table 4), P0.2-USY catalyzes the reaction pathway of glucose in ethanol to produce EMF in path I. P0.2-USY has a higher Lewis/ Brønsted acid ratio, which promotes the isomerization of glucose and benefits the production of EMF (He *et al*. 2022).

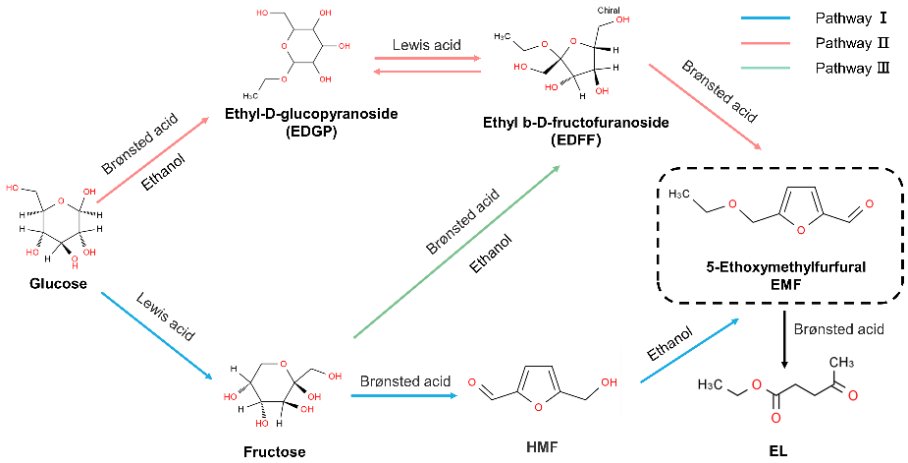

Fig. 9. The postulated reaction pathway of preparing EMF from glucose

Table 4. GC-MS Analysis Results of Glucose Ethanolysis into EMF

Retention time	P0.2-USY Identified compounds	USY Identified compounds	Molecular formula
1.485	Ether	-	$C_4H_{10}O$
2.52	3,5-Dioxaheptane	-	$C_5H_{12}O_2$
3.275	Acetal	Acetal	$C_6H_{14}O_2$
4.906	2-Furfural	2-Furfural	$C_5H_4O_2$
7.608	1,1,2-triethoxyethane	1,1,2-triethoxyethane	$C_8H_{18}O_3$
8.784	Ethyl levulinate	Ethyl levulinate	$C_7H_{12}O_3$
9.025	2-(Diethoxymethyl)furan	2-(Diethoxymethyl)furan	$C_9H_{14}O_3$
11.368	5-Hydroxymethylfurfural	5-Hydroxymethylfurfural	$C_6H_6O_3$
11.489	5-Ethoxymethylfurfural	5-Ethoxymethylfurfural	$C_8H_{10}O_3$
14.759	1,6-anhydro-β-D-glucose	1,6-anhydro-β-D-glucose	$C_6H_{10}O_5$
16.504	a-D-Glucopyranoside, ethyl	a-D-Glucopyranoside, ethyl	$C_8H_{16}O_6$
16.667	Methyl beta-D-glucopyranoside	Methyl beta-D-glucopyranoside	$C_7H_{14}O_6$

Kinetic Study of Glucose Conversion Reaction Catalyzed by P0.2-USY

In the ethanolysis process catalyzed by P0.2-USY, the conversion of glucose to EMF was the main reaction pathway. As discussed above, longer reaction times and higher temperature resulted in EL production and EMF decomposition, and some unknown by-products and humins were produced at the same time (Wang *et al*. 2022a). In this study, a pseudo-homogeneous first-order kinetics model was developed to reveal the glucose ethanolysis to EMF. As shown in Fig. 10, two parallel reactions existed in the reaction process: (1) ethanolysis of glucose to EMF and (2) conversion of glucose to unknown products and humins.

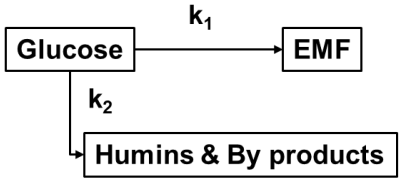

Fig. 10. Reaction kinetics model

The ethanolysis of glucose to EMF can be simplified to a first-order reaction, and the differential Eqs. 4 through 6 are obtained as follows,

$$\frac{dC_G}{dt} = -(k_1 C_G + k_2 C_G) \quad (4)$$

$$C_G = C_{G0} e^{-kt} \quad (5)$$

$$\frac{dC_{EMF}}{dt} = k_1 C_G = k_1 (C_{G0} e^{-kt}) \quad (6)$$

where CG is the glucose concentration ($g \cdot L^{-1}$) and the initial concentration is recorded as CG0; CEMF is the concentration of EMF ($g \cdot L^{-1}$); k_1 and k_2 are the reaction rate constants (min^{-1}) of EMF formation and by-products, respectively; k is the degradation reaction rate constant of glucose (min^{-1}), and t is the reaction time (min).

By solving Eq. 6, the EMF yield can be expressed as follows,

$$Y_{EMF} = \frac{k_1}{k_1 + k_2}\left[1 - e^{-(k_1+k_2)t}\right] \quad (7)$$

Figure 10 shows the variation of EMF yield with time, and the kinetic parameters were fitted by MATLAB based on the data in Fig. 11. The results are listed in Table 5. The rate constant increased with the increase of the temperature, indicating that high temperature promoted the ethanolysis of glucose. The rate constant for the conversion of glucose to EMF (k_1) was greater than the conversion of glucose to humins (k_2). Based on the reaction rate constant and the Arrhenius equation (Eq. 8), the activation energy (E_a, kJ·mol^{-1}) and exponential factor (A, min^{-1}) of each reaction stage was obtained. R is the gas constant (8.314 J mol^{-1} ·K^{-1}), and T is the temperature (K).

$$\ln k = \frac{-E_a}{RT} + \ln A \quad (8)$$

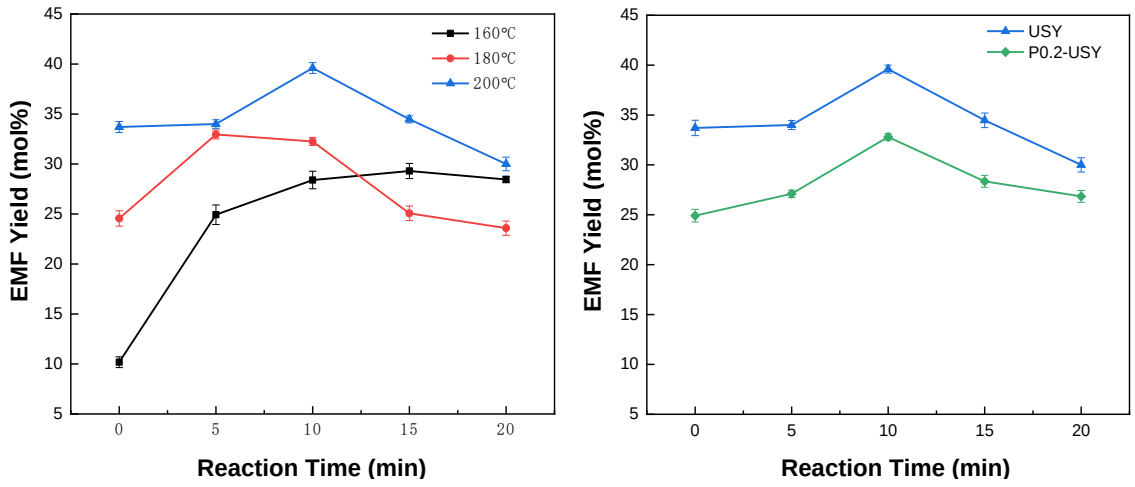

Fig. 11. (a) EMF yield over P0.2-USY at different temperatures. Reaction conditions: Substrate concentration 100 g·L^{-1}, Catalyst 1.95 wt% (b) EMF yield over USY and P0.2-USY. Reaction conditions: Substrate concentration 100 g·L^{-1}, Catalyst 1.95 wt%

The activation energies and pre-exponential factors of the reactions catalyzed by P0.2-USY are shown in Table 5. The value of E_{a1} (64.2 kJ·mol^{-1}) was lower than E_{a2} (73.2 kJ·mol^{-1}), showing that apparent activation energy for the conversion of glucose to EMF was lower than that for the conversion of glucose to humins and other by-products. This result indicated that EMF can be generated more easily than humins when P0.2-USY was used as the catalyst for glucose ethanolysis. As described in Fig. 12, the experimental data were in keeping with the theoretical data from the kinetics model, indicating that the kinetics of EMF formation was appropriately described by the kinetics model.

As shown in Table 6, the k_1 with P0.2-USY (0.2945 min^{-1}) catalyst was significantly higher than k_1 with USY(0.2103 min^{-1}) because P0.2-USY had a higher Lewis/ Brønsted acid ratio, which was more favorable for further alcoholysis of glucose isomerization to obtain EMF.

Table 5. Reaction Rate Constants and Kinetic Parameters for Glucose to EMF with P0.2-USY

Temperature (°C)	k_1/min^{-1}	k_2/min^{-1}
160	0.03606	0.05465
180	0.1985	0.5113
200	0.2945	0.5555
Parameter	Reaction	
	1	2
E_a (kJ·mol^{-1})	64.2	73.2
A (min^{-1})	0.299	0.558

Table 6. Reaction Rate Constants for Glucose to EMF with USY and P0.2-USY at 200 °C

	k_1/min^{-1}	k_2/min^{-1}
USY	0.2103	0.4985
P0.2-USY	0.2945	0.5555

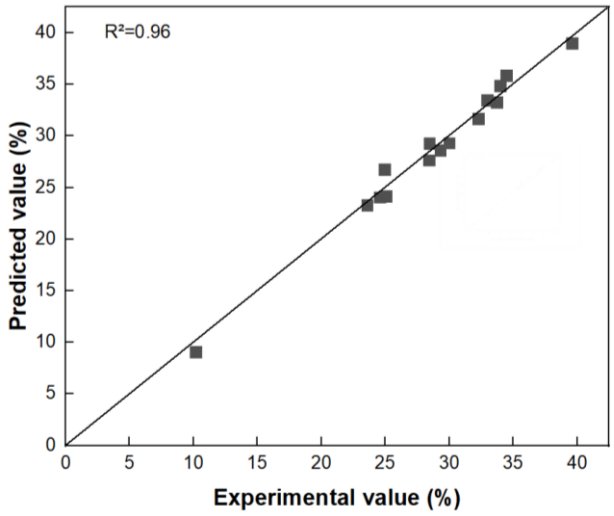

Fig. 12. Relation between predicted and experimental EMF yields

Comparison with Literature

To evaluate the advantages of the P0.2-USY catalyst, a comparison with recent study results of EMF preparation from glucose is shown in Table 6. In the ethanol medium (Table 7, entries 1 to 4), EMF yields were in the range of 32.8 to 41% in the presence of different catalysts. In the ethanol/water medium (Table 6, entries 5-8), the EMF yields were in the range of 18 to 33% with a small amount of HMF. Furthermore, the addition of DMSO to the reaction system (Table 6, entries 9-13) resulted in a long reaction time. In comparison, the high efficiency of the ethanol/THF reaction medium (Table 6, entries 9-13) may be attributed to the stabilization effect of THF on the EMF (Zhang *et al*. 2020). As shown in Table 6, the P0.2-USY showed a good catalytic performance, a comparable EMF yield can be obtained under the conditions of high substrate concentration and short reaction time, which can provide a strategy for the efficient production of EMF from glucose with high concentration.

Table 7. Comparison of Different Methods for the Synthesis of EMF from Glucose

Entry	Catalyst	Medium	Reaction Condition	EMF Yield (%)	Ref.
1	P0.2-USY	Ethanol	200 °C, 10 min, 100 g/L	39.6	This work
2	USY	Ethanol	200 °C, 10 min, 100 g/L	32.8	(Wang *et al*. 2022a)
3	Sn-STA/SBA-15	Ethanol	140 °C, 9 h, 45 g/L	41	(Srinivasa *et al*. 2020)
4	[BMIM][HSO_4]/$AlCl_3$	Ethanol	130 °C, 30 min	37	(Guo *et al*. 2018)
5	$AlCl_3$•$6H_2O$ and PTSA-POM	Ethanol/H_2O	150 °C, 30min, 44 g/L	30.6	(Xin *et al*. 2017)
6	$AlCl_3$•$6H_2O$	Ethanol/H_2O	160 °C, 15 min, 37 g/L	33	(Yang *et al*. 2012)
7	PCP(Cr)-BA	Ethanol/H_2O	140 °C, 22 h, 10 g/L	23.1	(Zhang *et al*. 2021)
8	PCP(Cr)-NA	Ethanol/H_2O	140 °C, 24 h, 10 g/L	18	
9	Al $(OTf)_3$	DMSO /H_2O	150 °C, 6 h, 36 g/L	20.6	(Yu *et al*. 2018)
10	Amberlyst-15 and Al $(OTf)_3$	DMSO /H_2O	150 °C, 6 h, 36 g/L	40.9	
11	Al $(DS)_3$	Ethanol/DMSO	160 °C,1 h, 30 g/L	37.9	(Mori *et al*. 2020)
12	Cr $(DS)_3$	Ethanol/DMSO	140 °C, 3 h, 30 g/L	22.1	
13	Glu-Fe_3O_4-SO_3H	Ethanol/DMSO	140 °C, 48 h	27	(Thombal and Jadhav 2016)
14	BFC-3	Ethanol/THF	100 °C, 10 h, 18 g/L	48.1	(Chen *et al*. 2020b)

CONCLUSIONS

The one-pot ethanolysis of glucose into 5-ethoxymethyl furfural (EMF) catalyzed by $NH_4H_2PO_4$ modified Ultra-stable Y (USY) zeolite P0.2-USY was investigated.

1. P0.2-USY exhibited a higher Lewis/Brønsted acid ratio which was effective for cascade isomerization-dehydration-etherification reactions.
2. P0.2-USY had a larger pore size and pore capacity, and it was possible to obtain a 39.6 mol% EMF yield at a high substrate concentration of 100 g/L, which is 20.7% higher than that catalyzed by USY.
3. The kinetic study showed that EMF formation had a higher reaction rate and smaller energy barrier than that of by-product formation.
4. P0.2-USY catalyzed fructose and corn straw can achieve better EMF yields which have good feasibility in biorefinery schemes.

5. The recycling test showed that P0.2-USY remained better activity after reused for 5 cycles.

ACKNOWLEDGMENTS

This study is supported by the National Natural Science Foundation of China (U1904122; 22178328), the Program of Processing and Efficient Utilization of Biomass Resources (GZS2022007) and the Henan Provincial Science and Technology Research Project (222102320059).

REFERENCES CITED

Bai, Y., Wei, L., Yang, M., Chen, H., Holdren, S., Zhu, G., Tran, D. T., Yao, C., Sun, R., Pan, Y., and Liu, D. (2018). "Three-step cascade over a single catalyst: Synthesis of 5-(ethoxymethyl)furfural from glucose over a hierarchical lamellar multi-functional zeolite catalyst," *Journal of Materials Chemistry A* 6(17), 7693-7705. DOI: 10.1039/c8ta01242c

Balakrishnan, M., Sacia, E. R., and Bell, A. T. (2012). "Etherification and reductive etherification of 5-(hydroxymethyl)furfural: 5-(Alkoxymethyl)furfurals and 2,5-bis(alkoxymethyl)furans as potential bio-diesel candidates," *Green Chemistry* 14(6), 1626-1634. DOI: 10.1039/c2gc35102a

Buttersack, C., and Laketic, D. (1994). "Hydrolysis of sucrose by dealuminated Y-zeolites," *Journal of Molecular Catalysis* 94(3), 283-290. DOI: 10.1016/0304-5102(94)00158-8

Chen, B., Xu, G., Chang, C., Zheng, Z., Wang, D., Zhang, S., Li, K., and Zou, C. (2019). "Efficient one-pot production of biofuel 5-ethoxymethylfurfural from corn stover: Optimization and kinetics," *Energy and Fuels* 33(5), 4310-4321. DOI: 10.1021/acs.energyfuels.9b00357

Chen, B., Yan, G., Chen, G., Feng, Y., Zeng, X., Sun, Y., Tang, X., Lei, T., and Lin, L. (2020a). "Recent progress in the development of advanced biofuel 5-ethoxymethyl-furfural," *BMC Energy* 2(1), 1-13. DOI: 10.1186/s42500-020-00012-5

Chen, Y., Guan, W., Zhang, Y., Yan, C., Li, B., Wei, Y., Pan, J., and Yan, Y. (2020b). "One-pot synthesis of the biofuel 5-ethoxymethylfurfural from carbohydrates using a bifunctional catalyst prepared through a pickering HIPE template and pore-filled strategy," *Energy and Fuels* 34(11), 14264-14274. DOI: 10.1021/acs.energyfuels.0c02942

Fals, J., García, J. R., Falco, M., and Sedran, U. (2020). "Performance of equilibrium FCC catalysts in the conversion of the SARA fractions in VGO," *Energy and Fuels* 34(12), 16512-16521. DOI: 10.1021/acs.energyfuels.0c02804

García, J. R., Falco, M., and Sedran, U. (2016). "Impact of the desilication treatment of y zeolite on the catalytic cracking of bulky hydrocarbon molecules," *Topics in Catalysis* 59(2-4), 268-277. DOI: 10.1007/s11244-015-0432-7

Gómez Millán, G., Hellsten, S., Llorca, J., Luque, R., Sixta, H., and Balu, A. M. (2019a). "Recent advances in the catalytic production of platform chemicals from holocellulosic biomass," *ChemCatChem* 11(8), 2022-2042. DOI: 10.1002/cctc.201801843

Gómez Millán, G., Phiri, J., Mäkelä, M., Maloney, T., Balu, A. M., Pineda, A., Llorca, J., and Sixta, H. (2019b). "Furfural production in a biphasic system using a carbonaceous solid acid catalyst," *Applied Catalysis A* 585. DOI: 10.1016/j.apcata.2019.117180

Guo, H., Duereh, A., Hiraga, Y., Qi, X., and Smith, R. L. (2018). "Mechanism of glucose conversion into 5-ethoxymethylfurfural in ethanol with hydrogen sulfate ionic liquid additives and a Lewis acid catalyst," *Energy and Fuels* 32(8), 8411-8419. DOI: 10.1021/acs.energyfuels.8b00717

He, Y., Zhang, L., Liu, Y., Yi, S., Yu, H., Zhu, Y., and Sun, R. (2022). "Sulfated complex metal oxides solid acids with dual Brønsted-Lewis acidic property for production of 5-ethoxymethylfurfural from biomass-derived carbohydrates," *Chemical Engineering Journal* 429, 132279. DOI: 10.1016/j.cej.2021.132279

Heda, J., Niphadkar, P., Mudliar, S., and Bokade, V. (2020). "Highly efficient micro-meso acidic H-USY catalyst for one step conversion of wheat straw to ethyl levulinate (biofuel additive)," *Microporous and Mesoporous Materials* 306, article 110474. DOI: 10.1016/j.micromeso.2020.110474

Kim, S. B., You, S. J., Kim, Y. T., Lee, S. M., Lee, H., Park, K., and Park, E. D. (2011). "Dehydration of D-xylose into furfural over H-zeolites," *Korean Journal of Chemical Engineering* 28(3), 710-716. DOI: 10.1007/s11814-010-0417-y

Li, H., Yang, S., Riisager, A., Pandey, A., Sangwan, R. S., Saravanamurugan, S., and Luque, R. (2016). "Zeolite and zeotype-catalysed transformations of biofuranic compounds," *Green Chemistry* 18(21), 5701-5735. DOI: 10.1039/c6gc02415g

Li, L., Quan, K., Xu, J., Liu, F., Liu, S., Yu, S., Xie, C., Zhang, B., and Ge, X. (2014). "Liquid hydrocarbon fuels from catalytic cracking of rubber seed oil using USY as catalyst," *Fuel* 123, 189-193. DOI: 10.1016/j.fuel.2014.01.049

Liu, X., and Wang, R. (2018). "Upgrading of carbohydrates to the biofuel candidate 5-ethoxymethylfurfural (EMF)," *International Journal of Chemical Engineering* 2018, 2316939. DOI: 10.1155/2018/2316939

Liu, X., and Wang, R. (2019). "5-Ethoxymethylfurfural-a remarkable biofuel candidate," *Biomass, Biofuels, Biochemicals* 355-375. DOI: 10.1016/B978-0-444-64307-0.00013-5

Liu, B., and Abu-Omar, M. M. (2021). "Lignin extraction and valorization using heterogeneous transition metal catalysts," *Advances in Inorganic Chemistry* 77, 137-174. DOI: 10.1016/bs.adioch.2021.02.001

Liu, J., Zhang, C., Song, D., Guo, Y., and Leng, J. (2021). "Efficient transformation of 5-hydroxymethylfurfural to ethyl levulinate over the Brønsted acidic ionic liquid functionalized dendritic fibrous nanosilica spheres," *Microporous and Mesoporous Materials* 326, 111354. DOI: 10.1016/j.micromeso.2021.111354

Morales, G., Paniagua, M., Melero, J. A., and Iglesias, J. (2017). "Efficient production of 5-ethoxymethylfurfural from fructose by sulfonic mesostructured silica using DMSO as co-solvent," *Catalysis Today* 279, 305-316. DOI: 10.1016/j.cattod.2016.02.016

Mori, Y., Katayama, Y., Shikata, T., and Kasuya, N. (2020). "Synthesis of 5-ethoxy-methylfurfural from saccharides using combined metal-surfactant catalyst in ethanol/dimethyl sulfoxide," *Research on Chemical Intermediates* 46(1), 609-620. DOI: 10.1007/s11164-019-03980-4

Nie, Y., Hou, Q., Qian, H., Bai, X., Xia, T., Lai, R., Yu, G., Rehman, M. L. U., and Ju, M. (2022). "Synthesis of mesoporous sulfonated carbon from chicken bones to boost rapid conversion of 5-hydroxymethylfurfural and carbohydrates to 5-ethoxymethyl-furfural," *Renewable Energy* 192, 279-288. DOI: 10.1016/j.renene.2022.04.105

Oruji, S., Khoshbin, R., and Karimzadeh, R. (2018). "Preparation of hierarchical structure of Y zeolite with ultrasonic-assisted alkaline treatment method used in catalytic cracking of middle distillate cut: The effect of irradiation time," *Fuel Processing Technology* 176(January), 283-295. DOI: 10.1016/j.fuproc.2018.03.035

Pande, A., Niphadkar, P., Pandare, K., and Bokade, V. (2018). "Acid modified H-USY zeolite for efficient catalytic transformation of fructose to 5-hydroxymethyl furfural (biofuel precursor) in methyl isobutyl ketone-water biphasic system," *Energy and Fuels* 32(3), 3783-3791. DOI: 10.1021/acs.energyfuels.7b03684

Peixoto, A. F., Ramos, R., Moreira, M. M., Soares, O. S. G. P., Ribeiro, L. S., Pereira, M. F. R., Delerue-Matos, C., and Freire, C. (2021). "Production of ethyl levulinate fuel bioadditive from 5-hydroxymethylfurfural over sulfonic acid functionalized biochar catalysts," *Fuel* 303(February), 121227. DOI: 10.1016/j.fuel.2021.121227

Srinivasa Rao, B., Dhana Lakshmi, D., Krishna Kumari, P., Rajitha, P., and Lingaiah, N. (2020). "Dehydrative etherification of carbohydrates to 5-ethoxymethylfurfural over SBA-15-supported Sn-modified heteropolysilicate catalysts," *Sustainable Energy and Fuels* 4(7), 3428-3437. DOI: 10.1039/d0se00509f

Thombal, R. S., and Jadhav, V. H. (2016). "Application of glucose derived magnetic solid acid for etherification of 5-HMF to 5-EMF, dehydration of sorbitol to isosorbide, and esterification of fatty acids," *Tetrahedron Letters* 57(39), 4398-4400. DOI: 10.1016/j.tetlet.2016.08.061

Tao, C., Peng, L., Zhang, J., and He, L. (2021). "Al-modified heteropolyacid facilitates alkyl levulinate production from cellulose and lignocellulosic biomass: Kinetics and mechanism studies," *Fuel Processing Technology* 213 (March). DOI: 10.1016/j.fuproc.2020.106709.

Verboekend, D., Vilé, G., and Pérez-Ramírez, J. (2012). "Hierarchical y and USY zeolites designed by post-synthetic strategies," *Advanced Functional Materials* 22(5), 916-928. DOI: 10.1002/adfm.201102411

Wang, J., Zhang, Z., Jin, S., and Shen, X. (2017). "Efficient conversion of carbohydrates into 5-hydroxylmethylfurfan and 5-ethoxymethylfurfural over sufonic acid-functionalized mesoporous carbon catalyst," *Fuel* 192, 102-107. DOI: 10.1016/j.fuel.2016.12.027

Wang, S., Chen, Y., Jia, Y., Xu, G., Chang, C., Guo, Q., Tao, H., Zou, C., and Li, K. (2021). "Experimental and theoretical studies on glucose conversion in ethanol solution to 5-ethoxymethylfurfural and ethyl levulinate catalyzed by a Brønsted acid," *Physical Chemistry Chemical Physics* 23, 19729-19739. DOI: 10.1039/d1cp02986j

Wang, S., Chen, Y., Jia, Y., Wang, C., Xu, G., Jiao, Y., He, C., Chang, C., and Guo, Q. (2022a). "DFT and dynamic analysis of glucose alcoholysis conversion to 5-ethoxy - methylfurfural and ethyl levulinate," *Fuel* 326(March), 125075. DOI: 10.1016/j.fuel.2022.125075

Wang, Y., Shi, J., Chen, X., Chen, M., Wang, J., and Yao, J. (2022b). "Ethyl levulinate production from cellulose conversion in ethanol medium over high-efficiency heteropoly acids," *Fuel* 324(May). DOI: 10.1016/j.2022.124642.

Wu, Q., Zhao, B., Liu, S., Yu, S., Huang, L., and Ragauskas, A. J. (2020). "From cellulose to 1,2,4-benzenetriolviacatalytic degradation over a wood-based activated carbon catalyst," *Catalysis Science and Technology* 10(10), 3423-3432. DOI: 10.1039/d0cy00424c

Xin, H., Zhang, T., Li, W., Su, M., Li, S., Shao, Q., and Ma, L. (2017). "Dehydration of glucose to 5-hydroxymethylfurfural and 5-ethoxymethylfurfural by combining Lewis and Brønsted acid," *RSC Advances* 7(66), 41546-41551. DOI: 10.1039/c7ra07684c

Xu, G., Chen, B., Zheng, Z., Li, K., and Tao, H. (2017). "One-pot ethanolysis of carbohydrates to promising biofuels: 5-ethoxymethylfurfural and ethyl levulinate," *Asia-Pacific Journal of Chemical Engineering* 12(4), 527-535. DOI: 10.1002/apj.2095

Yang, Y., Hu, C., and Abu-Omar, M. M. (2012). "Conversion of glucose into furans in the presence of AlCl 3 in an ethanol-water solvent system," *Bioresource Technology* 116, 190-194. DOI: 10.1016/j.biortech.2012.03.126

Yu, D., Liu, X., Jiang, J., Liu, Y., Tan, J., and Li, H. (2021). "Catalytic synthesis of the biofuel 5-ethoxymethylfurfural (EMF) from biomass sugars," *Journal of Chemistry* 2021, 9015481. DOI: 10.1155/2021/9015481

Yu, X., Gao, X., Peng, L., He, L., and Zhang, J. (2018). "Intensified 5-ethoxymethylfurfural production from biomass components over aluminum-based mixed-acid catalyst in co-solvent medium," *ChemistrySelect* 3(47), 13391-13399. DOI: 10.1002/slct.201803059

Zhang, Z., and Huber, G. W. (2018). "Catalytic oxidation of carbohydrates into organic acids and furan chemicals," *Chemical Society Reviews* 47(4), 1351-1390. DOI: 10.1039/c7cs00213k

Zhang, J., Dong, K., Luo, W., and Guan, H. (2018). "Catalytic Upgrading of Carbohydrates into 5-ethoxymethylfurfural using SO_3H functionalized hyper-cross-linked polymer based carbonaceous materials," *Fuel* 234(December). DOI:10.1016/j.fuel.2018.07.060

Zhang, L., Tian, L., Xi, G., Sun, R., and Zhao, X. (2020). "Catalytic valorization of expired fructan-rich food into the biofuel 5-ethoxymethylfurfural via a restaurant food waste-derived carbonaceous solid acid," *Waste and Biomass Valorization* 11(11), 6223-6233. DOI: 10.1007/s12649-019-00904-6

Zhang, L., Liu, Y., Sun, R., and Yi, S. (2021). "Sulfonic acid-functionalized PCP(Cr) catalysts with Cr^{3+} and $-SO_3H$ sites for 5-ethoxymethylfurfural production from glucose," *RSC Advances* 11(54), 33969-33979. DOI: 10.1039/d1ra05103b

Zheng, Z., Wang, C., Chen, Y., Wang, S., Guo, Q., Chang, C., Tao, H., and Xu, G. (2021). "One-pot efficient conversion of glucose into biofuel 5-ethoxymethylfurfural catalyzed by zeolite solid catalyst," *Biomass Conversion and Biorefinery*. DOI: 10.1007/s13399-021-01660-1

Article submitted: November 7, 2022; Peer review completed: December 10, 2022; Revised version received: January 4, 2023; Accepted: February 5, 2023; Published: February 9, 2023.
DOI: 10.15376/biores.18.2.2707-2725